Morpho-anatomical characterization and DNA barcoding of *Achillea millefolium* L.

**MOCHAMMAD ILHAM[1], SITI RIZQIYATUL MUKARROMAH[1], GALUH AYU RAKASHIWI[1],
DANI TRI INDRIATI[1], BRUNI FLARANDA YOKU[1], PUTUT RAKHMAD PURNAMA[2], JUNAIRIAH[1],
SEHANAT PRASONGSUK[1,3], HERY PURNOBASUKI[1], DWI KUSUMA WAHYUNI[1,3,♥]**

[1]Department of Biology, Faculty of Science and Technology, Universitas Airlangga. Jl. Dr. Ir. H. Soekarno, Surabaya 60115, East Java, Indonesia.
Tel.: +62-31-5936501, Fax.: +62-31-5936502, ♥email: dwi-k-w@fst.unair.ac.id
[2]Graduate Program in Bioinformatics and Computational Biology, Faculty of Science, Chulalongkorn University. 254 Phayathai Road, Wangmai,
Bangkok 10330, Thailand
[3]Department of Botany, Faculty of Science, Chulalongkorn University. 254 Phayathai Road, Wangmai, Bangkok 10330, Thailand

Manuscript received: 27 December 2021. Revision accepted: 23 March 2022.

Abstract. *Ilham M, Mukarromah SR, Rakashiwi GA, Indriati DT, Yoku BF, Purnama PR, Junairiah, Prasongsuk S, Purnobasuki H, Wahyuni DK. 2022. Morpho-anatomical characterization and DNA barcoding of* Achillea millefolium L. *Biodiversitas 23: 1958-1969.* One of the important things to study the distribution of secondary metabolites in the plant body is to carry out the identification process. Morphological markers have several limitations to recognize plants, therefore supporting data is needed so that the information becomes more comprehensive. This study aims to identify *Achillea millefolium* L. based on morphological, anatomical, and DNA barcoding markers to obtain specific data and avoid confusion. Morphological studies were carried out descriptively using vegetative organs, while anatomical studies of rhizomes, stems, and leaves used the paraffin method. The DNA barcoding was performed by analyzing genes from 3 different individuals. The research was carried out by amplifying and sequencing the partial gene in the *ribulose-bisphosphate carboxylase large subunit* (*rbcL*) regions and *maturase-K* (*matK*). The results showed that the plant had taproots, short stems due to root rosette and the leaves were double compound. The rhizome and stem tissues had almost the same structure, while the leaves had a tissue arrangement that was similar to other plants in general, except that the mesophyll tissue was undifferentiated. The results of DNA barcoding showed a percentage of identity above 98% for both the *rbcL* and *matK* genes.

Keywords: *Achillea millefolium,* DNA barcode, morpho-anatomy, *matK*, *rbcL*

Abbreviations: DNA: Deoxyribonucleic Acid, matK: maturase-K, rbcL: ribulose-bisphosphate carboxylase large subunit, CBOL: Consortium for Barcode of Life, PCR: Polymerase Chain Reaction, BLAST: Basic Local Alignment Search Tool

INTRODUCTION

Asteraceae is one of the largest angiosperm plant families, consisting of 26.000 species (Funk et al. 2009; Christenhusz and Byng 2016; Panero and Crozier 2016; Willis 2017). Daun seribu (*Achillea millefolium* L.) is a plant of the Asteraceae family that has potential in the medical field. The species is widespread in temperate regions of the Northern Hemisphere in Asia, Europe, and North America (Ugli and Parpiyev 2021). *A. millefolium* is commonly cultivated as an ornamental, in mountainous areas in some parts of Malesia and is naturalized locally there (Anonymous 2021). This plant has been used as herbal medicine since ancient Greece and used by native Americans (Baretta et al. 2012). Some studies have shown the presence of antioxidant and antibacterial activities present in essential oils in plants of the genus *Achillea,* such as Issabeagloo et al. (2012), Benedec et al. (2013), Mazandarani et al. (2013), Alfatemi et al. (2015), and Vitalini et al. (2016).

Secondary metabolites in plants are located explicitly in certain parts (Wahyuni et al. 2019). Most of the species belonging to the *Achillea* genus have been reported to contain flavonoids, such as *Achillea sintenisii* has phenolic compounds in the aerial part (Sabanoglu et al. 2017), and *A. millefolium* leaf extract contains flavonoids and phenolic compounds (Dusman et al. 2013). Yaseen et al. (2017) stated that the phenol content in the leaves of *A. millefolium* was greater than the stems. The difference in growing habitat may contribute to the varying quantities of secondary metabolite content in plants. Salomon et al. (2021) reported that *Achillea atrata* grown using artificial culture with those living in natural habitats have differences in the chemical compounds. *Achillea fragrantissima* which lives in two different areas in Saudi Arabia also contains different chemical compounds (Elsharkawy et al. 2020). Therefore, an anatomical study is required to understand the presence and location of cells that produce and store the secondary metabolites.

Study of plant anatomy can also be used for species identification, such as identification of 36 species of the Asteraceae family in Rajshahi can be distinguished based on the type of stoma, the location of the stomata, and the type of trichomes (Rahman et al. 2013). The existing anatomical study of *A. millefolium* is considered incomplete because it has not explained all parts of the plant. Each

species of the genus *Achillea* has the characteristics that distinguish it from the others, for example, 4 species of the genus *Achillea* in the western region of Ukraine have their characteristics, especially in the inflorescences, stems, and leaves (Grytsyk et al. 2016). The same *Achillea* species may have different morphology if they live in different places, such as *Achillea ageratifolia* which is limited to the Balkan peninsula is divided into 3 varieties/subspecies due to differences in habitat and geography (Franzen 1988).

The anatomical characteristics are important for the identification of species of pharmacological importance (Oliveira et al. 2020). Moreover, morphological characters also provide characteristics that can easily be used for identification (Widodo et al. 2014). However, morphological identification has many weaknesses, contemporary studies have shown that identification using morphological markers is highly dependent on environmental conditions and can result in variations in stature in different environments. This can lead to uncertainty of identification at the species level (Darienko et al. 2015). Morphological markers can either fail to discriminate species and mask the presence of cryptic species or discriminate different species while in reality there is only one (Duminil and Di Michele 2009). According to Sofiyanti et al. (2016) and Harsono et al. (2016), before DNA-based identification was often used, identification on plants was only based on morphological markers. To overcome ambiguity or misconceptions in species identification, it is possible to use molecular marker DNA barcoding (Imtiaz et al. 2017). DNA barcoding is a species identification method using short gene sequences from the genome of the organism (Kress et al. 2015). The CBOL Plant Working Group has proposed the use of 2 plastid molecular markers, such as *rbcL* (*ribulose-1,5-bisphosphate carboxylase*) and *matK* (*maturase K*) as standard barcodes (CBOL Plant Working Group 2009).

Plants identification will lead to ambiguous conclusions if only viewed from morphological markers, so other supporting data are needed, such as anatomy and DNA-based identification because this process is regarded as very important for understanding the biological mechanisms that exist in plants. This study aims to identify comprehensively based on morphological, anatomical, and DNA markers in *A. millefolium* plants. This investigation is expected to add important insights since *A. millefolium* has become a commodity for herbal medicine and medicinal products.

MATERIALS AND METHODS

Materials
The samples of *Achillea millefolium* were taken during September 2019 from the adult plants growing in the Taman Husada Graha Famili, Surabaya, Indonesia. Plant samples were taken as many as 3 individuals. The species identification was confirmed by comparing with herbarium collection in Purwodadi Botanical Garden, Indonesian Institute of Sciences, Pasuruan, Indonesia.

Morpho-anatomical characterization
Morphological characters were observed according to Akcin and Adnan (2010). However, this study focused on vegetative organs only, i.e. roots, stems, and leaves. The anatomical analysis was conducted according to Gregio and Moscheta (2006), the exception is that this study does not use roots. The anatomical characters observed were cells and structures found in cross-sectional preparations of rhizome, stems, and leaves. The anatomical preparations used the paraffin method. It is carried out by planting plant tissue in paraffin blocks to produce thin preparations. The preparation process using this method includes several procedures, namely cutting, fixation, aspiration, dehydration, dealcoholization, infiltration, embedding, trimming, staining, and mounting (Sari et al. 2016).

The process of making anatomical preparations begins with cutting plant tissue with a thickness of 0.5-1 cm. Pieces of plant tissue were fixed in FAA solution (Formalin, Glacial Acetic Acid, and 70% Alcohol) and simultaneously aspirated. Then, a dehydration process was carried out using graded alcohol (50%, 70%, 95%, and 100%) and a dealcoholization process using a clearing agent such as xylol. Then, the purification medium was replaced with a planting medium using paraffin that has been thawed with an incubator (infiltration). plant tissue was planted into paraffin blocks into solidifies, then the paraffin block will be shaped into a trapezium and will be cut using a microtome to produce a thin band. The paraffin band will be glued on a glass object that has been smeared with albumin. The last step is to color the thin paraffin band with safranin and fast green and cover the object-glass with a cover glass. Anatomical preparations will be observed under a light microscope to observe the tissues with magnificent 200-400x (Santos et al. 2016; Susetyarini et al. 2019).

DNA barcoding
DNA extraction
About 0.1 g fresh young leaves of *A. millefolium* were extracted using Plant DNA Genomic Kit (Tiangen, China) following the manufacturer's protocol. The purity and concentration of DNA samples were measured by Thermo Scientific Multiskan Go.

PCR amplification and sequencing
Amplification of the *rbcL* and *matK* genes using specific primers with the help of a PCR (Polymerase Chain Reaction) tool. Analysis of PCR was employed in two different primer pairs. Both primers *rbcL* (Forward: 5'AAGTTCCTCCACCGAACTGTAG 3'; Reverse: 5'TACTGCGGGTACATGCGAAG3') and *matK* (Forward: 5' TGGTTCAGGCTCTTCGCTATTG 3'; Reverse: 5'CTGATAAATCGGCCCAAATCGC 3') were previously used to barcode *Sonchus arvensis* (Wahyuni et al. 2019). The PCR mixtures were performed in a volume of 35 μL containing 7.5 μL GoTaq®Green Master Mix, each forward and reverse primers with a concentration of 350-500 nM, 50 ng^{-1} DNA template, and added with nuclease-free water until the solution volume up to 35 μL. The PCR cycle consists of 5 stages are as follows: pre-denaturation at 94°C for 5 min, 35 cycles of denaturation at

94°C for 30 sec, annealing at 56°C for 45 sec, extension at 72°C for 45 secs, and final extension at 72°C for 5 minutes.

To determine the quality and integrity of DNA that has been successfully amplified is through the process of electrophoresis. The PCR product of both genes was visualized using 1% agarose gel under a UV transilluminator and examined the presence of expected product PCR. Subsequently, the PCR products were performed sequencing at 1st Base Sequencing Service (Axil Scientific Pte. Ltd., Singapore).

Data analysis

Morpho-anatomical data will be analyzed descriptively. The DNA sequence of *rbcL* and *matK* region then was aligned using Bioedit 7.4 to obtain consensus data from forward and reverse sequences on each sample. Later, the multiple sequence alignment was performed using the DNA sequences of each sample against the Asteraceae sequences from the GenBank database using BLAST. The close kinship accessions of *A. millefolium* were obtained and subsequently used to reconstruct the phylogenetic tree using MEGA X software. In addition to using BLAST, several researchers use other software to align sequenced DNA such as ExPASy (Artimo et al. 2012) and MAFFT (Katoh and Sandley 2013).

The data used to construct the phylogenetic tree were data from 3 replicates of *A. millefolium* sequences and 20 sequences of plant data in the GenBank database that had the closest kinship to the sample (Table 1). Outgroup plants are selected based on the closest kinship value. Outgroups selected based on the *rbcL* gene were *Achillea* sp*., Achillea filipendulina, A. atrata, Tanacetum parthenium, T. cinerariifolium, T. coccineum, Anacyclus valentinus, A. pyrethrum, Formania mekongensis,* and *Anthemis cotula*. While the *matK* genes include *Achillea wilsoniana, A. ptarmica, Cota tinctoria, Tanacetum coccineum,* and *T. cinerariifolium*.

RESULTS AND DISCUSSION

Morpho-anatomy characterization

Based on morphological characteristics, *Achillea millefolium* is a perennial herbaceous plant (Figure 1A) (Modaresi and Delaram 2013; Noda et al. 2017; Majid et al. 2018). Its root system is taproot (Figure 1B) (Wahyuni et al. 2016) with long and light brown roots. Stems appear short due to the appearance of a rosette of roots, and this appearance is only seen in the vegetative phase (Gregio and Moscheta 2006). According to Grytsyk et al. (2016), *A. millefolium* has two types of stems, namely sterile and fertile stems. Sterile stems can be aerial stems that grow straight up (perpendicular). In addition, sterile stems can also be rhizomes that support vegetative propagation (horizontally in the ground) (Figures 1C and 1D). Fertile stems appear when entering the vegetative phase when in this stage the rosette appearance of the roots will disappear because the distance between the nodes is starting to be far apart. The nature of the stems of *A. millefolium* is like grass, growing upright with a hairy surface (Wahyuni et al. 2016).

The species has compound leaves of the bipinnatus or tripinnatus type, with the arrangement of leaves attached spirally to the stem (Figure 1E) as reported by Ali et al. (2017). Leaf margins of *A. millefolium* are curved (Gregio and Moscheta 2006). The leaflets have a blunt or rounded tip with a narrow leaf base (Figure 1F). The leaves are also almost covered by hairs with various levels of hair as reported by Ali et al. (2017). At first glance, the leaves of *A. millefolium* resemble the leaves of ferns (Wahyuni et al. 2016; Ayoobi et al. 2017), especially leaf buds that emerge from the aerial stems and appear to be curled (Figure 1G). Morphological research is only limited to vegetative organs because finding *A. millefolium* that enters the generative stage is very difficult.

Table 1. Plant data downloaded from GenBank

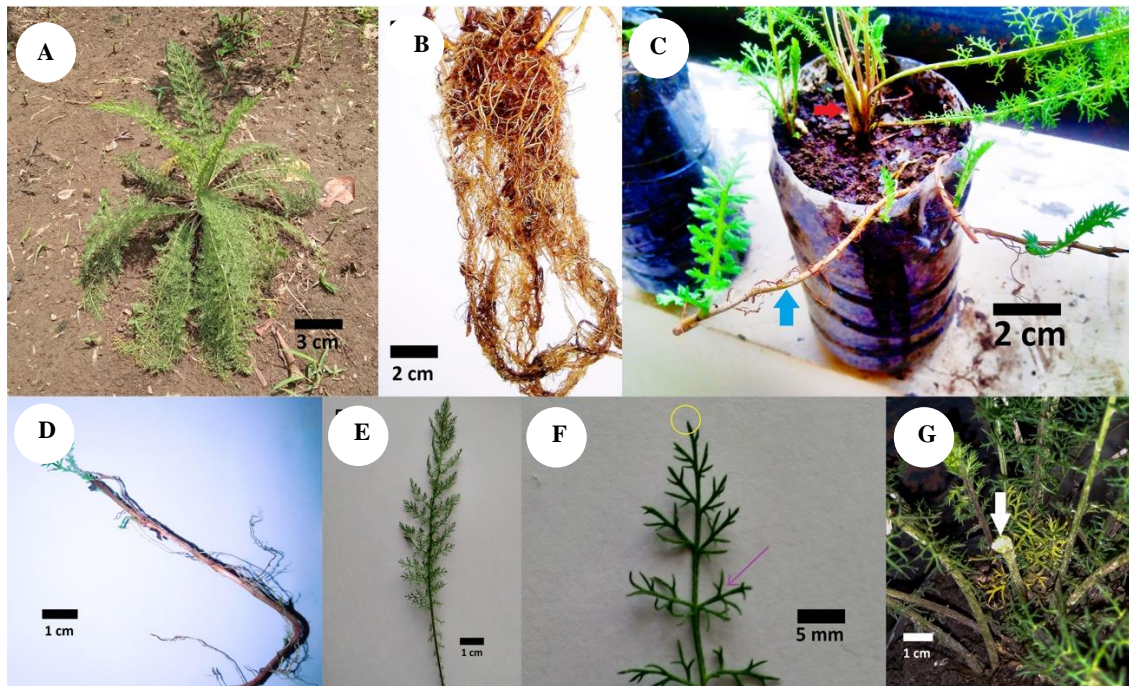| Plant (*rbcL*)	Accesion number (*rbcL*)	Plant (*matK*)	Accesion number (*matK*)
Achillea millefolium	MG946815.1	*Achillea millefolium*	KJ204429.1
Achillea millefolium	MN601429.1	*Achillea millefolium*	KX677563.1
Achillea millefolium	KP126894.1: 31723-33180	*Achillea millefolium*	KX676880.1
Achillea millefolium	KM360610.1	*Achillea millefolium*	KP126894.1: 1163-2677
Achillea millefolium	JX848399.1	*Achillea millefolium*	KJ204428.1
Achillea millefolium	HM849740.1	*Achillea millefolium*	EU385315.1
Achillea millefolium	EU384938.1	*Achillea millefolium*	KX677134.1
Achillea millefolium	L13641.1	*Achillea millefolium*	HM850607.1
Achillea millefolium	MH360736.1	*Achillea millefolium*	KX677060.1
Achillea filipendulina	AB530950.1	*Achillea millefolium*	MG946948.1
Achillea atrata	KF602245.1	*Achillea millefolium*	MF349876.1
Achillea sp.	MG946814.1	*Achillea millefolium*	MK509368.1
Tanacetum parthenium	HM850390.1	*Achillea wilsoniana*	HM989800.1
Tanacetum cinerariifolium	NC047309.1: 122194-123651	*Achillea ptarmica*	JN894397.1
Tanacetum coccineum	MT104463.1: 122148-123605	*Achillea ptarmica*	MK509369.1
Tanacetum coccineum	NC047308.1: 122148-123605	*Cota tinctoria*	KX677103.1
Anacyclus valentinus	GU817737.1	*Tanacetum coccineum*	NC047308.1:69393-70904
Anacyclus pyrethrum	MG946818.1	*Tanacetum coccineum*	MT104463.1:69393-70904
Formania mekongensis	KX527027	*Tanacetum cinerariifolium*	NC047309.1:69385-70896
Anthemis cotula	HM849779.1	*Tanacetum cinerariifolium*	MT104464.1:69385-70896

Figure 1. Morphology of vegetative organs of *Achillea millefolium*. A. habitus. B. roots. C. aerial stems (red arrows) and horizontal stems/rhizomes (blue arrows). D. rhizomes. E. compound leaves. F. leaf tips (yellow circle: leaf tip and purple arrow: leaf margin). G. leaf bud

Anatomical studies are very important to know the structure of cells, tissues, and organs that allow the synthesis of secondary metabolites (Sharma et al. 2017). Each organ has its characteristics in producing and storing its secondary metabolites. Anatomical observations of *A. millefolium* focused on rhizome, stem, and leaf tissue. The rhizome tissue in *A. millefolium* has a tissue structure that is almost similar to that of the stem tissue, because the rhizome is a modification of stem that grows below the surface of the soil (Indrani et al. 2020), except that the phloem fiber structure that appears intermittently (as in the stem) is not visible (Figures 2A and 2B).

The histology of *A. millefolium* stems (Figures 2C and 2D) is almost similar to *Achillea phrygia* and *A. gypsicola* described by Akcin and Adnan (2010). The stems of the studied plants are covered by the uniseriate epidermis. It is called uniseriate because it consists of a single layer of cells (Wulansari et al. 2020). The cells in the epidermis are rectangular. According to Karabourniotis et al. (2021), epidermis tissue generally consists of a compact layer with no intercellular spaces, under the prepared images which show no intercellular spaces. Collenchyma tissue is fused at the bottom of the epidermis, it's just that unlike the research by Akcin and Adnan (2010), The collenchyma tissue of the plant studied this time consists of a single layer with cells larger than the epidermis with irregular cortical shape and no chlorenchyma in between. In herbaceous plants, the collenchyma tissue is usually referred to as peripheral collenchyma (Driesen et al. 2021). Collenchyma serves to support plants without preventing cell elongation (Leroux 2012). The cortex is composed of multiple layers of parenchyma cells of various sizes arranged randomly, generally oval or rectangular. Unlike

the arrangement of cortical cells in *Achillea sivasica*, the arrangement of cells closer to the inside (endodermis) will increase in size (Tekin and Sedya 2021). The vascular bundle of this plant is of the open collateral type. This type of vascular bundle is also owned by some Asteraceae plants, such as *Pluchea lanceolata* (Khan et al. 2010), *Tragopogon dubius* (Moromete et al. 2014), genus *Tanacetum* (Tekin and Kartal 2016), *Artemisia monosperma,* and *Limbarda crithmoides* (El-Sherbeny et al. 2021). Vascular bundles of open collateral type are characterized by phloem which is always on the abaxial side of the xylem (Mehdi et al. 2019) and between them, there is a fascicular cambium. Phloem is composed of fibers and sieve tubes, the predominant structure seen is fiber. Pace (2019) explained that one of the constituents of phloem is sclerenchyma. It can be divided into fibers and sclereids. Cells in fibers have a long and slender shape while sclereids are composed of cells that are square or polygonal in shape with many pits found. Based on the observation, cell shape is longer and narrower with no pits, so it can be concluded that it is fiber. The fibers are arranged alternately to form a circle. Xylem is composed of the trachea with larger cell sizes and tracheids which have smaller cell sizes, similar to the results of Trueba et al. (2019) that the two xylem constituent elements have different sizes. In the innermost part of the stem, there is a pith tissue, this tissue consists of cells with the largest size when compared to other tissues in the stem and the arrangement of the cells is very tight. The pith is wide and consists of polygonal or oval parenchymatous cells although sometimes collapsed areas are observed in the center of stems (Karahan 2020). Pith parenchyma cells store water in various plant organs (Fujimoto et al. 2018).
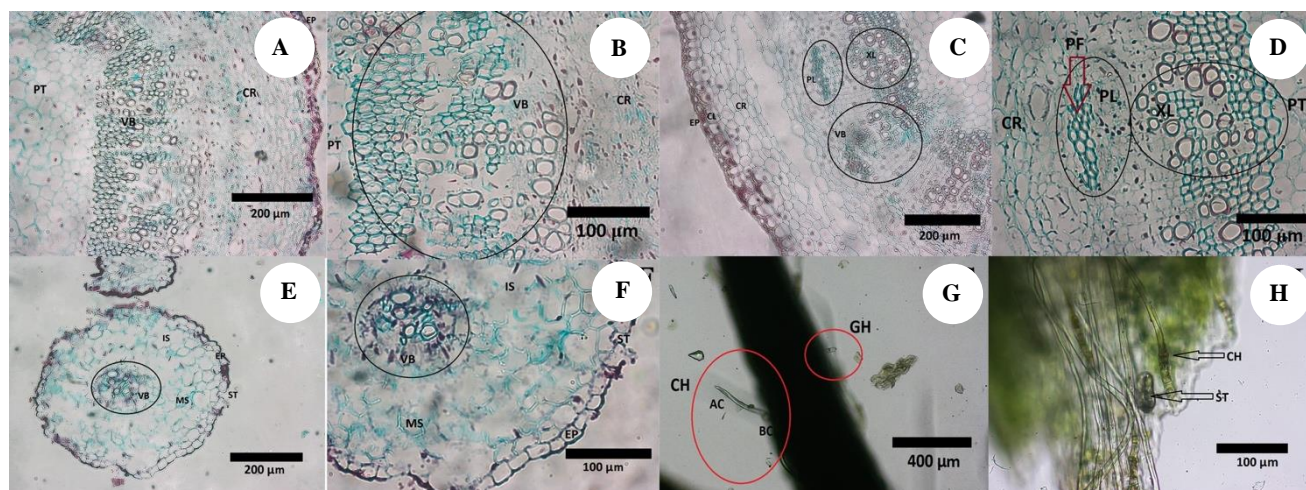
Figure 2. The anatomical structure of *Achillea millefolium* organ. A. rhizome 200x. B. rhizome 400x C. stem 200x. D. stem 400x. E. leaf 200x. F. leaf 400x. G. trichomes on leaves. H. trichomes and stomata on leaves. EP: epidermis, CL: collenchyma, CR: cortex, VB: vascular bundles, XL: xylem, PL: phloem, PF: phloem fibers, MS: mesophyll, IS: intercellular space, ST: stomata, CH: ceiling hairs, AC: apical cell, BC: basal cell, GH: glandular hair, PT: pith

The anatomical structure of *A. millefolium* leaves consists of epidermis, mesophyll tissue, and vascular bundles (Figures 2E and 2F). Epidermal tissue is composed of a single layer of cells with an oval or rectangular shape, and it is very similar to the epidermis of *A. gypsicola* leaves (Akcin and Adnan 2010). Mesophyll tissue consists of several layers of cells with the same shape (irregular shape) and the same type with lots of space between cells. It seems that the mesophyll tissue in *A. millefolium* is undifferentiated, unlike other Asteraceae species which have palisade and spongy tissues such as *A. phrygia*, *A. gypsicola* (Akcin and Adnan 2010), and *A. tracica* (Rogova et al. 2015). Another genus of the Asteraceae family also has differentiation in their mesophyll tissue as in *Senecio* (Nurhin et al. 2015). The vascular bundles are of the open collateral type. In the epidermal tissue, some gaps indicate the presence of stomata with an anomocytic type (Figures 2E, 2F, and 2H). This type of stomata is also found in *A. phrygia, A. gypsicola* (Akcin and Adnan 2010), *A. distans, A. stricta, A. carpatica* (Grytsyk et al. 2016), and *A. sivasica* (Tekin and Seyda 2021).

Achillea millefolium leaves have 2 kinds of trichomes, namely ceiling hairs and gland hairs (Figures 2G and 2H). Both types of trichomes were also identified by Gregio and Moscheta (2006) using the same plant. Trichomes gland hairs are also found in *A. filipendulina*, only the term is replaced with glandular trichomes (Afshari and Mehdi 2021). While *A. phrygia* and *A. gypsicola* have glandular trichomes (gland hairs) and eglandular trichomes (ceiling hairs) (Akcin and Adnan 2010). Ceiling hairs consist of basal cells at the bottom and apical cells at the top, apical cells have a pointed and elongated shape. Glandular hair consists of two basal cells, parallel to the epidermis, and eight oil-producing cells that are deposited under the cuticle (Gregio and Moscheta 2006).

DNA barcoding
PCR amplification and sequencing
The primer used in this study succeeded in amplifying the *rbcL* and *matK* genes with a size of approximately 500 bp (Figure 3A) and 750 bp (Figure 3B), respectively. According to Wahyuni et al. (2019), size of *rbcL* gene in *Sonchus arvensis* was not much different from the size of the gene belonging to *A. millefolium*, which was 433 bp. While in the *matK* gene there is a very large size difference, 288 base pairs. One of the determining factors for the success of PCR is the primer design (Yustinadewi et al. 2018). Primers can be designed using certain software, such as Primer-Blast (Ye et al. 2012). Annealing is the most important step in the PCR process, because at this stage an optimum temperature is required so that the DNA band is well amplified and also to facilitate DNA analysis (Nurjayadi et al. 2019) and at this stage, the primer is also attached to the DNA strand. In addition to primers and annealing, DNA concentration is also a factor supporting the success of PCR (Noflindawati et al. 2021).
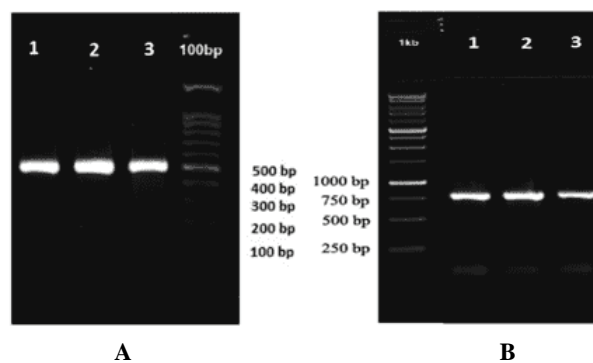

Figure 3. Results of electrophoresis visualization. A. *rbcL* gene. B. *matK* gene. 1: replicates 1, 2: replicates 2, and 3: replicates 3

The sequencing results of the *rbcL* gene showed 496 bp in replicates 1, 495 bp in replicates 2, and 494 bp in replicates 3. While the *matK* gene had a nucleotide count of 708 bp in replicates 1 and 2 and 709 bp in replicates 3 (Table 2). Sequencing results do not have too big a difference from the results of the electrophoresis visualization. DNA sequences obtained from this current study can be used to perform a match or alignment with DNA of organisms stored in the BOLD or NCBI libraries in just a few hours, so response times are highly dependent on available infrastructures, such as reference DNA sequences or available voucher specimens in NCBI and BOLD libraries (Imtiaz et al. 2017).

DNA sequence

Sequencing data shows that there is a gap in the *rbcL* gene in replicates 2 and 3, precisely at nucleotide number 8, and in replicates 3, there is a gap in nucleotide number 491 (Figure 4A). While in *matK* gene, the gap is at nucleotide number 30 (Figure 4B). The gaps appear in the *rbcL* and *matK* gene due to insertion or deletion events between nitrogen bases. The presence of gaps in DNA barcoding does not indicate a failure, instead, these gaps can be used to predict the success of DNA barcoding for the taxon being studied (Keskln and Atar 2013). The purpose of the sequence processing using the two software

(Bioedit dan MEGA) is to match homologous characters and to analyze the gaps in similar sequences.

The *rbcL* and *matK* genes in the plant being studied are compared with the complete genome coding sequence (CDS) of similar plants obtained from GenBank, then the position of the *rbcL* and *matK* genes in *A. millefolium* being studied is located around the middle area of the complete genome CDS (Figure 5). The *rbcL* gene is located at nucleotide number 241-736 relative to the complete genome CDS. While the *matK* gene is located at nucleotide number 840-1550 relative to the complete genome CDS.

The three samples studied had high similarity with the *A. millefolium* sequences in the GenBank database (Table 3). Percentage identity for the *rbcL* gene showed values of 98.99%, 99.19%, and 99.39%, while the *matK* gene had values of 99.86%, 99.86%, and 99.72%. Species having 70% or greater DNA similarity usually have more than 97% sequence identity (percentage identity) (Stackebrandt and Goebel 1994). Drancourt et al. (2000) state that identification can be confirmed at the species level if the percentage of similarity (percentage identity) is ≥99%. Choi et al. (2020) also stated that samples with a percentage similarity (percentage identity) greater than 97% compared to the available database sequences were considered the same species.

Table 2. The *rbcL* and *matK* genes sequencing of *Achillea millefolium*

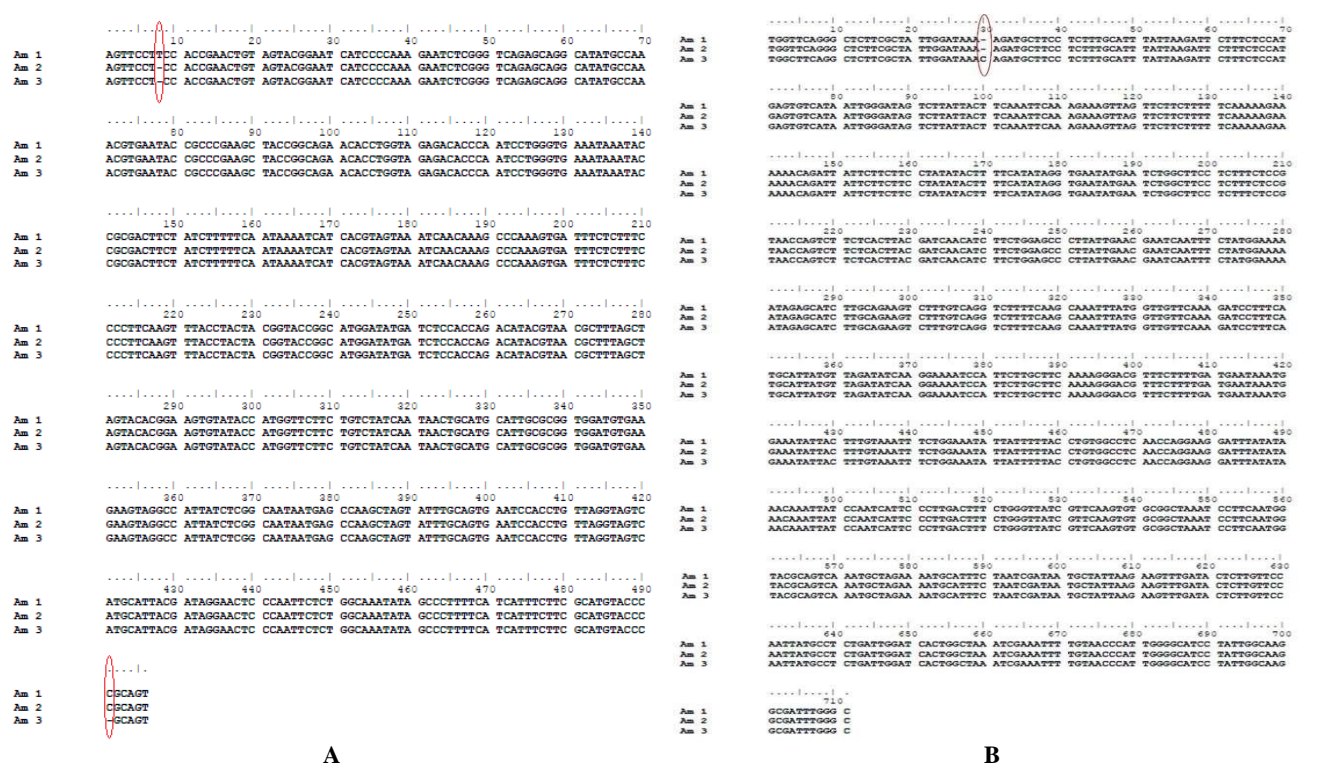| Plant	Sequence
A. millefolium rbcL 1	AGTTCCTTCCACCGAACTGTAGTACGGAATCATCCCCAAAGAATCTCGGGTCAGAGCAGGCATATGCCAAACGTGAATACCGCCCGAAGCTACCG GCAGAACACCTGGTAGAGACACCCAATCCTGGGTGAAATAAATACCGCGACTTCTATCTTTTTCAATAAAATCATCACGTAGTAAATCAACAAAG CCCAAAGTGATTTCTCTTTCCCCTTCAAGTTTACCTACTACGGTACCGGCATGGATATGATCTCCACCAGACATACGTAACGCTTTAGCTAGTACAC GGAAGTGTATACCATGGTTCTTCTGTCTATCAATAACTGCATGCATTGCGCGGTGGATGTGAAGAAGTAGGCCATTATCTCGGCAATAATGAGCCA AGCTAGTATTTGCAGTGAATCCACCTGTTAGGTAGTCATGCATTACGATAGGAACTCCCAATTCTCTGGCAAATATAGCCCTTTTCATCATTTCTTC GCATGTACCCCGCAGT (496)
A. millefolium rbcL 2	AGTTCCTCCACCGAACTGTAGTACGGAATCATCCCCAAAGAATCTCGGGTCAGAGCAGGCATATGCCAAACGTGAATACCGCCCGAAGCTACCGG CAGAACACCTGGTAGAGACACCCAATCCTGGGTGAAATAAATACCGCGACTTCTATCTTTTTCAATAAAATCATCACGTAGTAAATCAACAAAGC CCAAAGTGATTTCTCTTTCCCCTTCAAGTTTACCTACTACGGTACCGGCATGGATATGATCTCCACCAGACATACGTAACGCTTTAGCTAGTACACG GAAGTGTATACCATGGTTCTTCTGTCTATCAATAACTGCATGCATTGCGCGGTGGATGTGAAGAAGTAGGCCATTATCTCGGCAATAATGAGCCAA GCTAGTATTTGCAGTGAATCCACCTGTTAGGTAGTCATGCATTACGATAGGAACTCCCAATTCTCTGGCAAATATAGCCCTTTTCATCATTTCTTCG CATGTACCCCGCAGT (495)
A. millefolium rbcL 3	AGTTCCTCCACCGAACTGTAGTACGGAATCATCCCCAAAGAATCTCGGGTCAGAGCAGGCATATGCCAAACGTGAATACCGCCCGAAGCTACCGG CAGAACACCTGGTAGAGACACCCAATCCTGGGTGAAATAAATACCGCGACTTCTATCTTTTTCAATAAAATCATCACGTAGTAAATCAACAAAGC CCAAAGTGATTTCTCTTTCCCCTTCAAGTTTACCTACTACGGTACCGGCATGGATATGATCTCCACCAGACATACGTAACGCTTTAGCTAGTACACG GAAGTGTATACCATGGTTCTTCTGTCTATCAATAACTGCATGCATTGCGCGGTGGATGTGAAGAAGTAGGCCATTATCTCGGCAATAATGAGCCAA GCTAGTATTTGCAGTGAATCCACCTGTTAGGTAGTCATGCATTACGATAGGAACTCCCAATTCTCTGGCAAATATAGCCCTTTTCATCATTTCTTCG CATGTACCCCGCAGT (494)
A. millefolium matK 1	TGGTTCAGGGCTCTTCGCTATTGGATAAAAGATGCTTCCTCTTTGCATTTATTAAGATTCTTTCTCCATGAGTGTCATAATTGGGATAGTCTTATTAC TTCAAATTCAAAGAAAGTTAGTTCTTCTTTTTCAAAAAGAAAAAACAGATTATTCTTCTTCCTATATACTTTTCATATAGGTGAATATGAATCTGGC TTCCTCTTTCTCCGTAACCAGTCTTCTCACTTACGATCAACATCTTCTGGAGCCCTTATTGAACGAATCAATTTCTATGGAAAAATAGAGCATCTTG CAGAAGTCTTTGTCAGGTCTTTTCAAGCAAATTTATGGTTGTTCAAAGATCCTTTCATGCATTATGTTAGATATCAAGGAAAATCCATTCTTGCTTC AAAAGGGACGTTTCTTTTGATGAATAAATGGAAATATTACTTTGTAAATTTCTGGAAATATTATTTTTACCTGTGGCCTCAACCAGGAAGGATTTAT ATAAACAAATTATCCAATCATTCCCTTGACTTTCTGGGTTATCGTTCAAGTGTGCGGCTAAATCCTTCAATGGTACGCAGTCAAATGCTAGAAAAT GCATTTCTAATCGATAATGCTATTAAGAAGTTTGATACTCTTGTTCCAATTATGCCTCTGATTGGATCACTGGCTAAATCGAAATTTTTGTAACCCAT TGGGGCATCCTATTGGCAAGGCGATTTGGGC (708)
A. millefolium matK 2	TGGTTCAGGGCTCTTCGCTATTGGATAAAAGATGCTTCCTCTTTGCATTTATTAAGATTCTTTCTCCATGAGTGTCATAATTGGGATAGTCTTATTAC TTCAAATTCAAAGAAAGTTAGTTCTTCTTTTTCAAAAAGAAAAAACAGATTATTCTTCTTCCTATATACTTTTCATATAGGTGAATATGAATCTGGC TTCCTCTTTCTCCGTAACCAGTCTTCTCACTTACGATCAACATCTTCTGGAGCCCTTATTGAACGAATCAATTTCTATGGAAAAATAGAGCATCTTG CAGAAGTCTTTGTCAGGTCTTTTCAAGCAAATTTATGGTTGTTCAAAGATCCTTTCATGCATTATGTTAGATATCAAGGAAAATCCATTCTTGCTTC AAAAGGGACGTTTCTTTTGATGAATAAATGGAAATATTACTTTGTAAATTTCTGGAAATATTATTTTTACCTGTGGCCTCAACCAGGAAGGATTTAT ATAAACAAATTATCCAATCATTCCCTTGACTTTCTGGGTTATCGTTCAAGTGTGCGGCTAAATCCTTCAATGGTACGCAGTCAAATGCTAGAAAAT GCATTTCTAATCGATAATGCTATTAAGAAGTTTGATACTCTTGTTCCAATTATGCCTCTGATTGGATCACTGGCTAAATCGAAATTTTTGTAACCCAT TGGGGCATCCTATTGGCAAGGCGATTTGGGC (708)
A. millefolium matK 3	TGGCTTCAGGCTCTTCGCTATTGGATAAACAGATGCTTCCTCTTTGCATTTATTAAGATTCTTTCTCCATGAGTGTCATAATTGGGATAGTCTTATTA CTTCAAATTCAAAGAAAGTTAGTTCTTCTTTTTCAAAAAGAAAAAACAGATTATTCTTCTTCCTATATACTTTTCATATAGGTGAATATGAATCTGG CTTCCTCTTTCTCCGTAACCAGTCTTCTCACTTACGATCAACATCTTCTGGAGCCCTTATTGAACGAATCAATTTCTATGGAAAAATAGAGCATCTT GCAGAAGTCTTTGTCAGGTCTTTTCAAGCAAATTTATGGTTGTTCAAAGATCCTTTCATGCATTATGTTAGATATCAAGGAAAATCCATTCTTGCTT CAAAAGGGACGTTTCTTTTGATGAATAAATGGAAATATTACTTTGTAAATTTCTGGAAATATTATTTTTACCTGTGGCCTCAACCAGGAAGGATTTA TATAAACAAATTATCCAATCATTCCCTTGACTTTCTGGGTTATCGTTCAAGTGTGCGGCTAAATCCTTCAATGGTACGCAGTCAAATGCTAGAAAAT GCATTTCTAATCGATAATGCTATTAAGAAGTTTGATACTCTTGTTCCAATTATGCCTCTGATTGGATCACTGGCTAAATCGAAATTTTTGTAACCCAT TGGGGCATCCTATTGGCAAGGCGATTTGGGC (709)

Figure 4. The results of the alignment on the three replicates of *Achillea millefolium.* A. *rbcL* gene. B. *matK* gene. Am 1: replicates 1, Am 2: replicates 2, and Am 3: replicates 3. The red circle indicates a gap
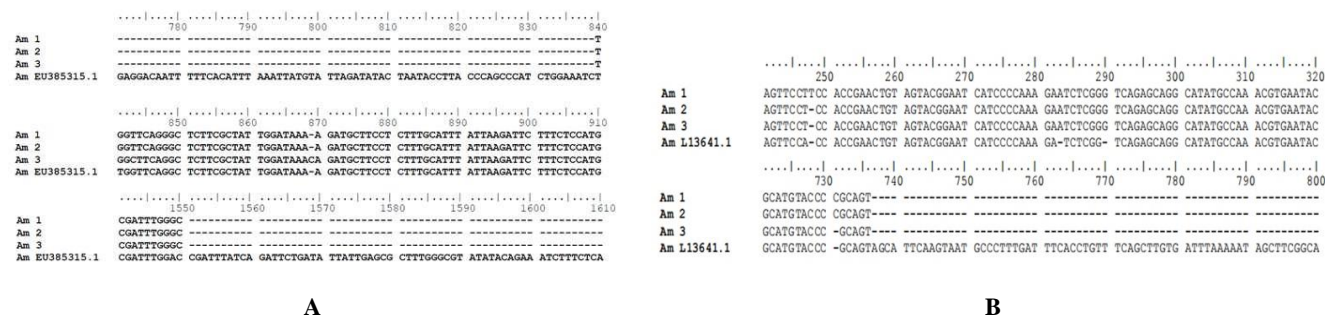

Figure 5. Comparison of *Achillea millefolium rbcL* and *matK* genes under investigation with the complete genome coding sequence (CDS) of *A. millefolium* from the GenBank database. A. The *rbcL* gene compared with the complete genome CDS of *A. millefolium* L13641.1. B. The *matK* gene compared with the complete genome CDS of *A. millefolium* EU385315.1. Am 1: replicates 1, Am 2: replicates 2, and Am 3: replicates 3

Table 3. Alignment results of *Achillea millefolium* using BLAST

| Replicates | Value | | | | | GenBank sequence |
	Max. score	Total score	Query cover	E-value	Per. identity	
rbcL						
replicates *rbcL* 1	885	885	100 %	0.0	98.99 %	*A. millefolium* MN601429.1
replicates *rbcL* 2	889	889	100 %	0.0	99.19 %	*A. millefolium* MN601429.1
replicates *rbcL* 3	894	894	100 %	0.0	99.39 %	*A. millefolium* MN601429.1
matK						
replicates *matK* 1	1301	1301	99 %	0.0	99.86 %	*A. millefolium* MG946948.1
replicates *matK* 2	1301	1301	99 %	0.0	99.86 %	*A. millefolium* MG946948.1
replicates *matK* 3	1297	1297	99 %	0.0	99.72 %	*A. millefolium* MG946948.1

The query cover shows a value of 100% for the *rbcL* gene and 99% for the *matK* gene, which means that the sample DNA sequences aligned with the DNA sequence in the GenBank have identical nucleotides in length. If the query cover has a higher percentage value, the homology level between the 2 specimens will also be high (Nugraha et al. 2014) According to Sogandi (2018), the e-value of 0 indicates that the DNA sequence of the sample with the sequence in the GenBank database is identical, this is following the results of the BLAST analysis (Table 3), that the e-value of all samples is 0.0 which indicates that the sample similar to *A. millefolium* registered in the GenBank database.

As standards for plant DNA barcodes, *rbcL* and *matK* genes have several advantages, such as providing many characters for phylogenetic studies, and high success rates with one or two universal primers (CBOL Plant Working Group 2009). The *rbcL* gene function is to code for the RuBisCO protein and it has a low mutation rate so that the intraspecies similarity level is quite high (Asahina et al. 2010). This low level of mutation provides benefits for in-depth study of intraspecies genetic and phylogenetic variations (Sundari et al. 2019). According to Estevez et al. (2015), *rbcL* has been shown to vary widely enough to distinguish most land plant species. *matK* gene has a high evolutionary rate and this sequence is highly variable, so it is often used for molecular plant identification and phylogenetic studies (Patwardhan et al. 2014; Guo et al. 2016). The gene can be used to distinguish a species, easily sequenced, easily amplified to produce a good nucleotide sequence (Hollingsworth et al. 2011), and had higher individual discrimination and barcode success compared with *rbcL* (Biswab et al. 2019). In addition to *rbcL* and *matK* genes, chloroplast-based genes such as ITS2 can identify *A. millefolium* well (Newmaster et al. 2013).

Phylogenetic analysis

The phylogenetic tree was built based on data from 3 sample sequences and 20 sequences from the GenBank database (Figure 6). The phylogenetic tree shows the replicates of *A. millefolium* under study were located in the same clade with the same branch length. Identical branch lengths between taxa groups indicate no sequence changes within a species. If the value of branch length is greater, then there are more sequence or evolutionary changes that occur (Hall 2001; Zein and Sulandari 2009), while the shorter line indicates the close evolutionary distance between species (Anafarida and Badruzsaufari 2020). The branch inhabited by the studied sample has a close distance to the branch inhabited by sequences from the GenBank, the majority of which are in the same species. The plants being studied are not 100% similar to some of the *A. millefolium* sequences found in the GenBank database. There are differences in their nitrogen bases, although to a very small degree. This very small difference is due to the mutation and recombination rate of the chloroplast genome being much lower compared to the nuclear genome, which results in fewer repeat sequences and transposons (Neiman and Taylor 2009; Smith 2015). Phylogenetic trees generated by *rbcL* and *matK* genes (Figures 6A and 6B)

have fundamental differences. The relationship between taxa *A. millefolium* in the *matK* gene is not specific or not very close, which is characterized by several branches of *A. millefolium* that have different branch lengths and some of them are not present in the same clade. This might be because the taxa discriminatory ability of the *matK* gene is better than that of the *rbcL* gene. While in the *rbcL* gene, most of the *A. millefolium* groups were located in the same clade and had the same branch length. Sun et al. (2012) reported that *matK* successfully identified 23.26% species of the genus *Dioscorea*, *rbcL* had a percentage of 9.30% and 11.63% in *psbA-trnH*. Therefore, *matK* is recommended as the best DNA barcoding candidate, because it has a good discriminating ability. The *matK* gene has a high discrimination efficiency in plant identification, because it shows better resolution of the phylogenetic tree when compared to the phylogenetic tree reconstructed from other genes such as *rbcL* (Bafeel et al. 2012). According to Olivar et al. (2014), the *rbcL* gene has low interspecific discriminatory ability, but very high intraspecific divergence. Therefore, *rbcL* can illustrate that similar species have the same branch length and are located in the same clade (Figure 6A).

In addition, Li (2011) stated that plastid DNA barcoding loci might not be able to discriminate between closely related species within a genus. They posited that the low performance of *rbcL* in this parameter is attributed to the low mutation rate of bases in plastid DNA markers. Almost all *A. millefolium* species in the phylogenetic tree, both from *rbcL* and *matK* genes, are known to come from different geographic areas (countries) from the sample plants and indicate differences in genetic distance. It can be concluded that there is a relationship between geographic barriers and genetic diversity. Schmitt and Haubrich (2008) and Laltanpuii et al. (2014) stated that the greater the value of the genetic distance between populations or individuals, the more isolated they are from one another, genetic distance indicates the possible influence of geographic isolation on a population. According to Yang et al. (2013), the development of each species under the influence of a certain environment, natural ecosystem, and socio-economic have caused each species to have or develop its specific genetic character. The close distance between branches is directly proportional to the close relationship between taxa. Plants with different genera but still in the same family Asteraceae (genus *Tanacetum*) have branch positions that are quite far from the branches inhabited by the sample plants.

Plants with different genera but still in a similar family, such as *Tanacetum cinerariifolium*, *T. coccineum*, and *T. parthenium* have branch positions that are quite far from the branches inhabited by the sample plants. In addition to having a fairly far branch distance and not close kinship with the sample plants, the sequences of these plants when compared with the sample plants have some differences in their nucleotide variations. The comparison of the *rbcL* gene shows a gap in the *Tanacetum* sequence at nucleotides numbers 248, 283, 290, and 731. While the nucleotide variations (different nucleotide sequences) can be found in nucleotides number 247, 364, 442, 480, 646, 670 (Figure

7A). The comparison of the *matK* gene shows a gap in the *Tanacetum* sequence at nucleotide number 495 only, while the nucleotide variations can be found in nucleotides number 467, 469, 471, 472, 473, 641, 844, 901, 915, 1142, and 1175 (Figure 7B).
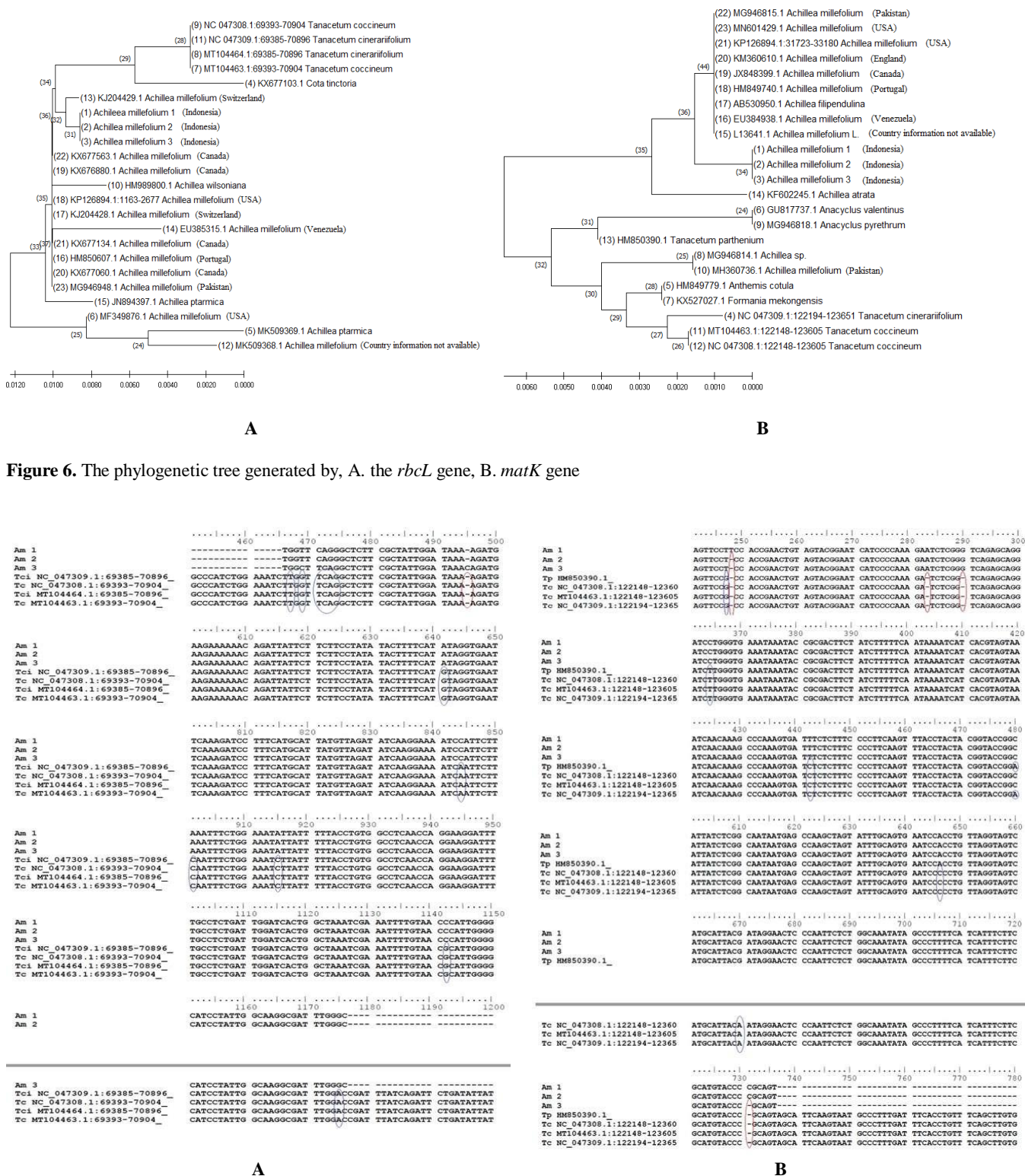
Figure 6. The phylogenetic tree generated by, A. the *rbcL* gene, B. *matK* gene

Figure 7. Comparison between *Achillea millefolium* sequence studied with several species of the genus *Tanacetum*. A. *rbcL* gene. B. *matK* gene. Am 1: replicates 1, Am 2: replicates 2, and Am 3: replicates 3, Tci: *Tanacetum cinerariifolium*, Tc: *Tanacetum coccineum*, Tp: *Tanacetum parthenium*. A red circle indicates a gap, blue circle indicates the presence of different nucleotides (variations)

It can be concluded that based on morphological observations, *A. millefolium* had a taproot with short stems due to the appearance of a rosette of roots and leaves of bipinnatus or tripinnatus type. On anatomical observation, the rhizome had a tissue that was almost similar to the stem. While the leaf anatomy had leaf tissue found in plants of the Asteraceae family in genera, the mesophyll tissue was undifferentiated. The DNA alignment and reconstruction of the phylogenetic tree revealed that the studied plant had a very high relationship with *A. millefolium* which was registered in the GenBank database.

ACKNOWLEDGEMENTS

REFERENCES

Afshari M, Mehdi R. 2021. Variation in essential oil composition, anatomical, and antioxidant characteristics of *Achillea filipendulina* Lam. as affected by different phenological stages. J Essent Oil Res 33 (3): 283-298. DOI: 10.1080/10412905.2021.1885510.

Akcin TA, Adnan. 2010. Morphological and anatomical characteristics and taxonomical significance of achene micromorphology of *Achillea phrygia* and *A. gypsicola* (Asteraceae), endemic to Turkey. Nordic J Bot 28: 65-73. DOI: 10.1111/j.1756-1051.2009.00464.x.

Alfatemi SM, Rad JS, Rad MS, Mohsenzadeh S, da Silva JA. 2015. Chemical composition, antioxidant activity and in vitro antibacterial activity of *Achillea wilhelmsii* C. Koch essential oil on methicillin-susceptible and methicillin-resistant *Staphylococcus aureus* spp. 3 Biotech 5 (1): 39-44. DOI: 10.1007/s13205-014-0197-x.

Ali SI, Gopalakrishnan B, Venkatesalu V. 2017. Pharmacognosy, phytochemistry and pharmacological properties of *Achillea millefolium* L.: A review. Phytother Res 31 (8): 1140-1161. DOI: 10.1002/ptr.5840.

Anafarida O, Badruzsaufari. 2020. Philogenetic analysis of mango (*Mangifera* spp.) based on 5.8s RNA gene. Ziraa'ah 45 (2): 120-126. DOI: 10.31602/zmip.v45i2.3001.

Anonymous. 2021. Daun seribu (Yarrow: *Achillea millefolium*). https://rempahid.com/achillea-millefolium/.

Artimo P, Jonnalagedda M, Arnold K, Baratin D, Csardi G, de Castro E, Duvaud S, Flegel V, Fortier A, Gasteiger E, Grosdidier A, Hernandez C, Ioannidis V, Kuznetsov D, Liechti R, Moretti S, Mostaguir K, Redaschi N, Rossier G, Xenarios I, Stockinger H. 2012. ExPASy: SIB bioinformatics resource portal. Nucl. Acids Res 40 (W1): 597-603. DOI: 10.1093/nar/gks400.

Asahina H, Shinozaki J, Masuda K, Morimitsu Y. 2010. Identification of medicinal *Dendrobium* species by phylogenetic analyses using *matK* and *rbcL* sequences. J Nat Med 64: 133-138. DOI: 10.1007/s11418-009-0379-8.

Ayoobi F, Shamsizadeh A, Fatemi I, Vakilian A, Allahtavakoli M, Hassanshahi G, Moghadam-Ahmadi A. 2017. Bio-effectiveness of the main flavonoids of *Achillea millefolium* in the pathophysiology of neurodegenerative disorders-a review. Iran J Basic Med Sci 20 (6): 604-612.

Bafeel S, Arif I, Al-Homaidan A, Khan H, Ahamed A, Bakir N. 2012. Assessment of DNA barcoding for the identification of *Chenopodium murale* L. (Chenopodiaceae). Intl J Biol 4 (4): 66-74. DOI: 10.5539/ijb.v4n4p66.

Baretta IP, Felizardo RA, Bimbato VF, dos Santos MG, Kassuya CA, Gasparotto Junior A, da Silva CR, de Oliveira SM, Ferreira J, Andreatini R. 2012. Anxiolytic-like effects of acute and chronic treatment with *Achillea millefolium* L. extract. J Ethnopharmacol 140 (1): 46-54. DOI: 10.1016/j.jep.2011.11.047.

Benedec D, Vlase L, Oniga I, Mot AC, Damian G, Hanganu D, Duma M, Silaghi-Dumitrescu R. 2013. Polyphenolic composition, antioxidant and antibacterial activities for two Romanian subspecies of *Achillea distans* Waldst. et Kit. ex Willd. Molecules 18 (8): 8725-8739. DOI: 10.3390/molecules18088725.

Biswab R, Anindya SR, Rahib B. 2019. In silico analyses of burial codon bias among the species of Dipterocarpaceae through molecular and phylogenetic data. Evol Bioinforma 15: 1-12. DOI: 10.1177/1176934319834888.

CBOL Plant Working Group. 2009. A DNA Barcode for land plants. Proc Natl Acad Sci USA 106 (31): 12794-12797. DOI: 10.1073/pnas.0905845106.

Choi JH, Jeong DG, Oh JN, Kim S, Lee YH, UngChoi Y, Myoung JG, Kim CG. 2020. DNA barcoding of coral reef fishes from Chuuk State, Micronesia. Mitochondrial DNA B: Resour 5 (3): 3733-3738. DOI: 10.1080/23802359.2020.1831981.

Christenhusz MJM, Byng JW. 2016. The number of known plants species in the world and its annual increase. Phytotaxa 261: 201-217. DOI: 10.11646/phytotaxa.261.3.1.

Darienko T, Gustavs L, Eggert A, Wolf W, Pröschold T. 2015. Evaluating the species boundaries of green microalgae (Coccomyxa, Trebouxiophyceae, Chlorophyta) using integrative taxonomy and DNA barcoding with further implications for the species identification in environmental samples. PLoS One 10 (6): e0127838. DOI: 10.1371/journal.pone.0127838.

Drancourt M, Bollet C, Carlioz A, Martelin R, Gayral JP, Raoult D. 2000. 16S ribosomal DNA sequence analysis of a large collection of environmental and clinical unidentifiable bacterial isolates. J Clin Microbiol 38 (10): 3623-3630. DOI: 10.1128/JCM.38.10.3623-3630.2000.

Driesen E, De Proft M, Saeys W. 2021. Soil moisture levels affect the anatomy and mechanical properties of basil stems (*Ocimum basilicum* L.). Plants 10 (7): 1320. DOI: 10.3390/plants10071320.

Duminil J, Di Michele M. 2009. Plant species delimitation: A comparison of morphological and molecular markers. Plants Biosyst 143: 528-542. DOI: 10.1080/11263500902722964.

Dusman E, de Almeida IV, Coelho AC, Balbi TJ, Dusman Tonin LT, Vicentini, VE. 2013. Antimutagenic effect of medicinal plants *Achillea millefolium* and *Bauhinia forficata* in vivo. Evid Based Complement Alternat Med 2013: 893050. DOI: 10.1155/2013/893050.

Elsharkawy ER, Alghanem SM, Elmorsy E. 2020. Effect of habitat variations on the chemical composition, antioxidant, and antimicrobial activities of *Achillea fragrantissima* (Forssk) Sch. Bip. Biotechnol Rep (Amst) 29: e00581. DOI: 10.1016/j.btre.2020.e00581.

El-Sherbeny GA, Dakhil MA, Eid EM, Abdelaal M. 2021. Structural and chemical adaptations of *Artemisia monosperma* Delile and *Limbarda crithmoides* (L.) Dumort. In response to arid coastal environments along the Mediterranean Coast of Egypt. Plants 10 (3): 481. DOI: 10.3390/plants10030481.

Estevez I, Mensah S, Tian R, Fein M. 2015. DNA barcoding and phylogenetic analysis of plant species: Urban barcode project of New York city. Intl J Sci Res Sci Eng Technol 1 (4): 347-352.

Franzen R. 1988. Differentiation patterns in *Achillea ageratifolia* (Asteraceae). Willdenowia 18 (1): 47-62.

Fujimoto M, Sazuka T, Oda Y, Kawahigashi H, Wu J, Takanashi H, Ohnishi T, Yoneda JI, Ishimori M, Kajiya-Kanegae H, Hibara KI, Ishizuna F, Ebine K, Ueda T, Tokunaga T, Iwata H, Matsumoto T, Kasuga S, Yonemaru JI, Tsutsumi N. 2018. Transcriptional switch for programmed cell death in pith parenchyma of sorghum stems. Proc Natl Acad Sci USA 115 (37): E8783-E8792. DOI: 10.1073/pnas.1807501115.

Funk VA, Susana A, Stuessy TF, Bayer RJ. 2009. Systematics, Evolution and Biogeography of Compositae. Smithsonian Institution, Washington D.C.

Gregio SDJD, Moscheta, EIS. 2006. Anatomia de raiz, caule e folha e identificação de estruturas. Maringá 28 (4): 327-334. DOI: 10.4025/actascibiolsci.v28i4.163.

Grytsyk AR, Neiko OV, Melnyk MV. 2016. Morphological-anatomical study of *Achillea* L. species in western region of Ukraine. Pharma Innovation 5 (1): 71-73.

Guo YY, Huang LQ, Liu ZJ, Wang XQ. 2016. Promise and challenge of DNA barcoding in Venus slipper (*Paphiopedilum*). PLoS One 11 (1): e0146880. DOI: 10.1371/journal.pone.0146880.

Hall BG. 2001. Phylogenetic Trees Made Easy: A How – To Manual for Molecular Biologists. Sinauer Associates, Inc. Sunderland, Massachusetts.

Harsono T, Pasaribu N, Sobir, Fitmawati. 2016. Diversity of gandaria (*Bouea*) based on morphological characters in Indonesia. SABRAO J Breed Genet 48 (4): 504-517.

Hollingsworth PM, Graha SW, Little DP. 2011. Choosing and using a plant DNA barcode. PLoS One 6 (5): e19254. DOI: 10.1371/journal.pone.0019254.

Imtiaz A, Siti AZMN, Darlina MDN. 2017. Review: Progress and potential of DNA barcoding for species identification of fish species. Biodiversitas 18 (4): 1394-1405. DOI: 10.13057/biodiv/d180415.

Indrani K, Khrisne D, Suyadnya I. 2020. Android based application for rhizome medicinal plant recognition using squeezenet. J Electr Electron Inform 4 (1): 10-14. DOI: 10.24843/JEEI.2020.v04.i01.p02.

Issabeagloo E, Taghizadieh M, Abri B. 2012. Antimicrobial effects of yarrow (*Achillea millefolium*) essential oils against *Staphylococcus* species. Afr J Pharm Pharmacol 6 (41): 2895-2899. DOI: 10.5897/AJPP12.397.

Karabourniotis G, Liakopoulos G, Bresta P, Nikolopoulos D. 2021. The optical properties of leaf structural elements and their contribution to photosynthetic performance and photoprotection. Plants 10 (7): 1455. DOI: 10.3390/plants10071455.

Karahan M. 2020. Morphology, anatomy, palynology and achene micromorphology of *Bellis* L. (Asteraceae) species from Turkey. Acta Bot Croat 79 (1): 59-67. DOI: 10.37427/botcro-2020-006.

Katoh K, Standley DM. 2013. MAFFT multiple sequence alignment software version 7: Improvements in performance and usability. Mol Biol Evol 30 (4): 772-780. DOI: 10.1093/molbev/mst010.

Keskİn E, Atar HH. 2013. DNA barcoding commercially important fish species of Turkey. Mol Ecol Resour 13 (5): 788-797. DOI: 10.1111/1755-0998.12120.

Khan S, Rawat R, Rawat AKS, Shirwaiker A. 2010. A report on the quality control parameters of aerial parts of *Pluchea lanceolata* (DC.) Oliv. & Hiern, Asteraceae. Braz J Pharmacogn 20 (4): 563-567. DOI: 10.1590/S0102-695X2010000400015.

Kress WJ, Garcia-Robledo C, Uriate M, Erickson DL. 2015. DNA barcodes for ecology, evolution, and conservation. Trends Ecol Evol 30 (1): 25-35. DOI: 10.1016/j.tree.2014.10.008.

Laltanpuii N, Kumar S, Mathai MT. 2014. Molecular and phylogenetic analysis of the genus *Orthetrum* (Odonata: Anisoptera: Libellulidae) using Mitochondrial COI gene. Sci Vis 14 (3): 152-257.

Leroux O. 2012. Collenchyma: A versatile mechanical tissue with dynamic cell walls. Ann Bot 110 (6): 1083-1098. 10.1093/aob/mcs186

Li DZ. 2011. Comparative analysis of a large dataset indicates that internal transcribed spacer (ITS) should be incorporated into the core barcode for seed plants. Proc Natl Acad Sci USA 108 (49) 19641-19646. DOI: 10.1073/pnas.1104551108.

Mazandarani M, Mirdeilami ZS, Pessarakli M. 2013. Essential oil composition and antibacterial activity of *Achillea millefolium* L. from different regions in North East of Iran. J Med Plant Res 7 (16): 1063-1069.

Mehdi R, Christian EL, Ravi BA, Christina M, Muhammad S, Janine K, Max EK, Frank L, Michael K, Wilhelm G, Uwe S, Wolfgang Z. 2019. Symplasmic phloem unloading and radial post-phloem transport via vascular rays in tuberous roots of *Manihot esculenta*. J Exp Bot 70 (20): 5559-5573. DOI: 10.1093/jxb/erz297.

Majid M, Mudasir R, Lubna A, Mohmad IB. 2018. *Achillea millefolium* L.: A promising health aid in modern pharmacology. Intl J Adv Res Sci Eng 7 (4): 2167-2182.

Modaresi M, Delaram D. 2013. The effects of yarrow's (*Achillea millefolium*) hydroalcoholic extract on bloodproteins in mice. Nat Environ Pollut Technol 12 (2): 281-284.

Moromete C, Mariana A, Laura B, Natalia R. 2014. General data regarding *Tragopogon dubius* scop. Species – Pharmacognostic analysis. Ser Ştiinţele Vieţii 24 (4): 399-405.

Neiman M, Taylor DR. 2009. The causes of mutation accumulation in mitochondrial genomes. Proc Biol Sci 276: 1201-1209. DOI: 10.1098/rspb.2008.1758.

Newmaster SG, Grguric M, Shanmughanandhan D, Ramalingam S, Ragupathy S. 2013. DNA barcoding detects contamination and substitution in North American herbal products. BMC Medicine 11: 222. DOI: 10.1186/1741-7015-11-222.

Nurjayadi M, Efrianti UR, Azizah N, Julio E, Nastassya L, Saamia V. 2019. Optimum temperature of the amplification of the fljB gene of *Salmonella typhimurium*. In: Rahmawati Y, Taylor PC (Eds.). Empowering Science and Mathematics for Global Competitiveness. 1st Edition. CRC Press, London.

Noda K, Eisuke K, Jun K. 2017. Intestinal α-Glucosidase inhibitors in *Achillea millefolium*. Nat Prod Commun 12 (8): 1259-1261. DOI: 10.1177/1934578X1701200828.

Noflindawati, Anwar A, Sutanto A, Yusniwati. 2021. Optimization of annealing cycle and temperature SNAP T12 primer distinguishing markers for male, female and hermaphrodite plants in papaya (*Carica papaya* L). IOP Conf Ser: Earth Environ Sci 715 (1): 012040. DOI: 10.1088/1755-1315/715/1/012040.

Nugraha F, Indriyani D, Ardilla Y, Herman. 2014. Analysis of partial gene sequence ferritin2 on rice plants (*Oryza sativa* L.) Indragiri Hilir, Riau. Biosaintifika 6 (2): 70-79.

Nurhin HB, Hatice C, Umit B. 2015. Stem and leaf anatomy and achene structure in some species of *Senecio* (Asteraceae). Ann Plant Sci 6 (12): 1845-1854. DOI: 10.21746/aps.2017.6.12.7.

Olivar JEC, Brillantes RY, Rubite RR, Alejandro GJD. 2014. Evaluation of three candidate DNA barcoding loci in selected *Ficus* L. (Moraceae). Intl J Sci Technol Res 3 (9): 43-48.

Oliveira CF, Vinicius BO, Vanessa BO, Katlin SR, Fernando CMB, Josiane FGD, Sandra MWZ, Obdulio GM, Marilis DM. 2020. Phytochemical and morpho-anatomical study of the vegetative organs of *Psychotria fractistipula* L.B.Sm., R.M. Klein & Delprete (Rubiaceae). Braz J Pharm Sci 56: e18158. DOI: 10.1590/s2175-97902020000118158.

Pace MR. 2019. Phloem: Cell types, structure, and commercial uses. In: Gonzales AM, Rodriguez M, Saglam NG (Eds.). Plant Science-Structure, Anatomy and Morphogenesis in Plants Cultured in vivo and in vitro. IntechOpen Limited, London.

Panero JL, Crozier BS. 2016. Macroevolutionary dynamics in the early diversification of Asteraceae. Mol Phylogen Evol 99: 116-132. DOI: 10.1016/j.ympev.2016.03.007.

Patwardhan A, Ray SK, Roy A. 2014. Molecular markers in phylogenetic studies: A review. J Phylogenetics Evol Biol 2: 131. DOI: 10.4172/2329-9002.1000131.

Rahman AHM, Islam AKM, Rahman M.. 2013. An anatomical investigation on Asteraceae family at Rajshahi Division, Bangladesh. Intl J Biosci 3 (1): 13-23. DOI: 10.11648/j.plant.20130102.11.

Rogova M, Gnewa TS, Stefanova M, Koleva D, Toteva VK. 2015. Morphoanatomical study of in vitro propagated and ex vitro adapted *Achillea thracica* Velen. Plants Bulg. J Agric Sci 21 (5): 947-950.

Sabanoglu M, Elian K, Gulcin S, Mehmet T, Burcin BA. 2017. Secondary Metabolites of *Achillea sintenisii* HUB. MOR. Fabad J Pharm Sci 42 (3): 191-197.

Salomon L, Lorenz P, Ehrmann B, Spring O, Stintzing FC, Kammerer DR. 2021. Impact of environmental conditions on growth and the phenolic profile of *Achillea atrata* L. Processes 9 (5): 853. DOI: 10.3390/pr9050853.

Santos RF, Barbara MN, Rafaela DS, Luis ALS, Karina PR. 2016. Morpho-anatomical study of *Ageratum conyzoides*. Rev Bras Farmacogn 26: 679-687. DOI: 10.1016/j.bjp.2016.07.002.

Sari DP, Fatmawati U, Prabasari RM. 2016. Profile of hands on activity in microtechnical courses. Proc Biol Educ Conf 13 (1): 476-481.

Schmitt T, Haubrich K. 2008. The genetic structure of the mountain forest butterfly *Erebia euryale* unravels the late pleistocene and postglacial history of the mountain coniferous forest biome in Europe. Mol Ecol 17 (9): 2194-2207. DOI: 10.1111/j.1365-294X.2007.03687.x.

Sharma S, Richa, Harsimran. 2017. Phytochemical and anatomical screening of *Eclipta prostrata* L. an important medical herb from Chandigarh. J Med Plants Stud 5 (2): 255-258.

Smith DR. 2015. Mutation rates in plastid genomes: They are lower than you might think. Genome Biol Evol 7: 1227-1234. DOI: 10.1093/gbe/evv069.

Sofiyanti N, Mat–Salleh K, Mahmud K, Mazlan NZ, Hasein MRA, Burslem DFRP. 2016. *Rafflesia parvimaculata* (Rafflesiaceae), a new species of *Rafflesia* from Peninsular Malaysia. Phyotaxa 253 (3): 207-213. DOI: 10.11646/phytotaxa.253.3.4.

Sogandi. 2018. Molecular Biology for Molecular Identification of Bacteria. Universitas 17 Agustus 1945, Jakarta.

Stackebrandt E, Goebel B. 1994. Taxonomic note a place for DNA-DNA reassociation and 16S rRNA sequence analysis in the present species definition in bacteriology. Intl J Syst Bacteriol 44: 846-849. DOI: 10.1099/00207713-44-4-846.

Sun XQ, Zhu YJ, Guo JL, Peng B, Bai MM, Hang YY. 2012. DNA barcoding the *Dioscorea* in China, a vital group in the evolution of monocotyledon: use of *matK* gene for species discrimination. PLoS One 7 (2): e32057. DOI: 10.1371/journal.pone.0032057.

Sundari, Khadijah, Jayali AM, Sukamto NH. 2019. The application of barcode DNA *rbcL* gene for identification of medicinal plants: Red jabon and gofasa. J Phys Conf Ser 1146 (1): 012030. DOI: 10.1088/1742-6596/1146/1/012030.

Susetyarini E, Poncojari W, Roimil L, Endrik N. 2019. The Identification of morphological and anatomical structures of *Pluchea indica*. J Phys Conf Ser 1539: 012001. DOI: 10.1088/1742-6596/1539/1/012001.

Tekin M, Kartal C. 2016. Comparative anatomical investigations on six endemic *Tanacetum* (Asteraceae) taxa from Turkey. Pak J Bot 48 (4): 1501-1515.

Tekin M, Seyda A. 2021. Anatomical investigations of the Turkish critically endangered species: *Achillea sivasica* Çelik et Akpulat (Asteraceae). Acta Bot Croat 80 (1): 91-98. DOI: 10.37427/botcro-2021-006.

Trueba S, Delzon S, Isnard S, Lens F. 2019. Similar hydraulic efficiency and safety across vesselless Angiosperms and vessel-bearing species with scalariform perforation plates. J Exp Bot 70: 3227-3240. DOI: 10.1093/jxb/erz133.

Ugli NMHG, Parpiyev ATU. 2021. Some flavonoids in the yarrow (*Achillea millefolium* L.) plant and their effects on human health. Am J Soc Human Res 2 (5): 116-120.

Vitalini S, Madeo M, Tava A, Iriti M, Vallone L, Avato P, Cocuzza CE, Simonetti P, Argentieri MP. 2016. Chemical profile, antioxidant and antibacterial activities of *Achillea moschata* Wulfen, an endemic species from the Alps. Molecules 21 (7): 830. DOI: 10.3390/molecules21070830.

Wahyuni DK, Ekasari W, Witono JR, Purnobasuki H. 2016. TOGA Indonesia. Airlangga University Press, Surabaya.

Wahyuni DK, Rahayu S, Purnama PR, Saputro TB, Suharyanto, Wijayanti N, Purnobasuki H. 2019. Morpho-anatomical structure and DNA barcode of *Sonchus arvensis* L. Biodiversitas 20 (8): 2417-2426. DOI: 10.13057/biodiv/d200841.

Widodo, Mohamad A, Mimien HIA, Muhammad JL. 2014. Morpho-anatomical analysis of *Cosmostigma racemosum* (Asclepiadoideae) flowers. Biol Medic Nat Prod Chem 3 (1): 35-46. DOI: 10.14421/biomedich.2014.31.35-46.

Willis KJ. 2017. State of the World's Plants 2017: Report. Royal Botanic Gardens, Kew.

Wulansari TYI, Esthi LA, Eka FT, Widoyanti. 2020. Anatomical structure of leaves as evidence in delimiting the taxon of flowering plants: case studies of 12 Indonesian flowering plant family. Buletin Kebun Raya 23 (2): 146-161.

Yang W, Kang X, Yang Q, Lin Y, Fang M. 2013. Review on the development of genotyping methods for assessing farm animal diversity. J Anim Sci Biotechnol 4 (1): 2. DOI: 10.1186/2049-1891-4-2.

Yaseen M, Mudasar A, Tareq AW, Manzoor A, Gani BA, Rashida Q. 2017. Phytochemical screening and antioxidant activity of extracts of the leaf and stem of *Achillea millefolium*. Intl J Adv Sci Res 2 (6): 55-59.

Ye J, Coulouris G, Zaretskaya I, Cutcutache I, Rozen S, Madden TL. 2012. Primer-BLAST: A tool to design target-specific primers for polymerase chain reaction. BMC Bioinform 13: 134. DOI: 10.1186/1471-2105-13-134.

Yustinadewi, Yustiantara PS, Narayani I. 2018. Primary design technique for the Mdr-1 gene sequence variant 1199 in buffy coat samples of pediatric patients with LLA. J Metamorf 5 (1): 105-111. DOI: 10.24843/metamorfosa.2018.v05.i01.p16.

Zein MSA, Sulandari S. 2009. Pedigree investigation of Indonesian chicken by sequences hypervariable-1 d-loop mitochondrial DNA. J Vet 10 (1): 41-49.